

# Formation of Ti-Aluminides on Commercially Pure Ti via the Hot-Dipping Aluminizing Process

Sinan Aksöz<sup>1</sup> · Yavuz Kaplan<sup>2</sup>

Received: 24 December 2019 / Accepted: 9 March 2020 / Published online: 24 March 2020  
© The Indian Institute of Metals - IIM 2020

**Abstract** This study examined the applicability of the hot-dipping aluminizing technique carried out on commercially pure titanium (Ti) as a new method for the formation of Ti-aluminides on a Ti surface. The process was carried out using pure aluminum (Al) and Al 7075 alloy in molten Al baths at 900 °C and 1000 °C for 4 h and 6 h, respectively. The microstructure, phase fraction, and composition analysis of the formed layers were examined using field emission scanning electron microscopy, energy-dispersive spectroscopy, and X-ray diffraction. Three different areas with different thicknesses were formed on the Ti surface by the hot-dipping aluminizing technique. The top (Al coating) layer consisted of Ti and Al elements having a higher hardness than the base metal. The second layer, formed below the Al coating, was the Ti–Al layer having the highest hardness on the surface. Below this layer the Al was diffused. As a result of the Ti aluminizing process carried out at different temperatures and durations in this study, TiAl, TiAl<sub>2</sub>, TiAl<sub>3</sub>, and Ti<sub>3</sub>Al phases were obtained. These phases positively affected the mechanical and corrosion properties.

**Keywords** Aluminizing · Ti-aluminides · Intermetallics · Microhardness

## 1 Introduction

Titanium (Ti) and Ti alloys possess a great combination of desirable material properties, such as high corrosion resistance, high specific strength, low density, and excellent biocompatibility [1, 2]. These properties enable the usage of Ti in the aerospace, marine, chemical, power, and automotive industries [3, 4]. In addition, the TiO<sub>2</sub> layer on the Ti surface exhibits strong corrosion passivity at temperatures up to 500 °C. However, at temperatures exceeding 500 °C, the oxidation resistance of Ti greatly decreases and continues to decrease at a rate parallel to the increasing temperature, eventually losing its protection against oxygen, nitrogen, and hydrogen embrittlement [5, 6].

The oxidation resistance of Ti can be improved with surface treatments. Many studies have been conducted on surface treatments to enhance the oxidation and corrosion resistance of Ti and Ti alloys; some of these include overlay coating [7, 8], pack cementation [9, 10], thermal coatings produced by plasma spraying techniques [11, 12]. However, the poor adhesion of these coatings to the substrate is the main problem [13]. They are also difficult to apply on complex-shaped surfaces, and therefore, a simpler and cheaper method is desired.

Aluminizing is an excellent candidate for the surface modification of Ti alloys, because it provides a protective aluminide layer not only in air, but, due to the high thermodynamic stability of the aluminide layers, also in aggressive corrosive environments containing H<sub>2</sub>O, SO<sub>2</sub>, and H<sub>2</sub>S [14–16]. The hot-dipping parameters can be affected in particular by the processing time, substrate, bath composition, and temperature. Thus, the microstructure, thickness of the layer, construction of the phases, and also the hardness values obtained during the aluminizing

✉ Sinan Aksöz  
saksoz@pau.edu.tr

<sup>1</sup> Faculty of Technology, Department of Metallurgical and Materials Engineering, Pamukkale University, Pamukkale, Turkey

<sup>2</sup> Faculty of Technology, Department of Mechanical and Manufacturing Engineering, Pamukkale University, Pamukkale, Turkey

process can change during the service, depending upon the duration and temperature of the oxidation [14, 17, 18].

The Ti-aluminides possess attractive physical, chemical, and mechanical properties along with low density, which make them ideal candidates for application as structural materials in the aerospace industry [19, 20]. However, their use on an industrial scale is hampered by various natural challenges, mostly seen as being related to their synthesis [21]. Moreover, conventional techniques that essentially consist of long-term thermal treatments do not facilitate the production of homogeneous intermetallic phases [22]. Their formation is prevented by contemporary nucleation and growth of the TiAl and Ti<sub>3</sub>Al phases, which are often thermodynamically stable [23–25].

The purpose of this study was to determine the details of the formation of the Ti-aluminide phases: TiAl, TiAl<sub>2</sub>, TiAl<sub>3</sub>, and Ti<sub>3</sub>Al, by using the hot-dipping aluminizing (H-DA) process on a commercially pure (CP) Ti surface. In order to determine the effects of the H-DA process on a Ti alloy, different temperatures and times were used as parameters and the obtained structures were characterized via field emission scanning electron microscopy (FESEM), energy-dispersive spectroscopy (EDS), and X-ray diffraction (XRD) analyses. The H-DA process used in this study provided unique TiAl, TiAl<sub>2</sub>, TiAl<sub>3</sub>, and Ti<sub>3</sub>Al phases for the formation of aluminide coatings on Ti alloys. Accordingly, these structures could be widely applied commercially.

## 2 Experimental Procedure

The commercially pure (CP) Ti (Grade-1) cylindrical specimens,  $\varnothing 10 \times 20$  mm, were coated in an Al 7075 bath and a pure Al bath using the H-DA technique. A schematic illustration of the process is shown in Fig. 1. The composition of Al 7075 is given in Table 1. The process was carried out at 900 °C and 1000 °C for 4 h and 6 h, respectively, to form Ti-aluminides on the surface. All processes were carried out in an argon (Ar) atmosphere to avoid any contamination problems.

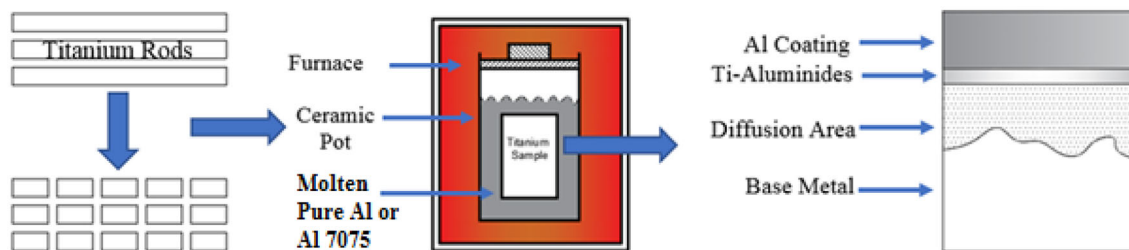


**Fig. 1** Schematic illustration of hot-dipping aluminizing

Following the H-DA process, the specimens were grinded with coarse- and fine-grit SiC paper and then polished using 6- $\mu\text{m}$ , 3- $\mu\text{m}$ , and finally 1- $\mu\text{m}$  diamond paste. After polishing, the samples were etched with Kroll's reagent.

The examination of the aluminide layers was carried out via the ZEISS SUPRA 40 VP model FESEM equipped with an elemental dispersion spectrometer (EDS). The XRD analyses were used to determine the intermetallic phases in the microstructure and coating.

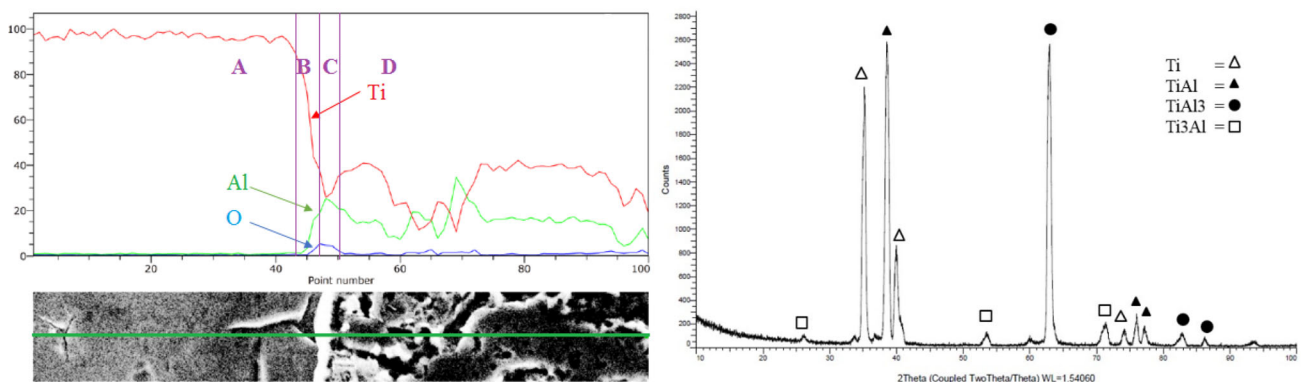
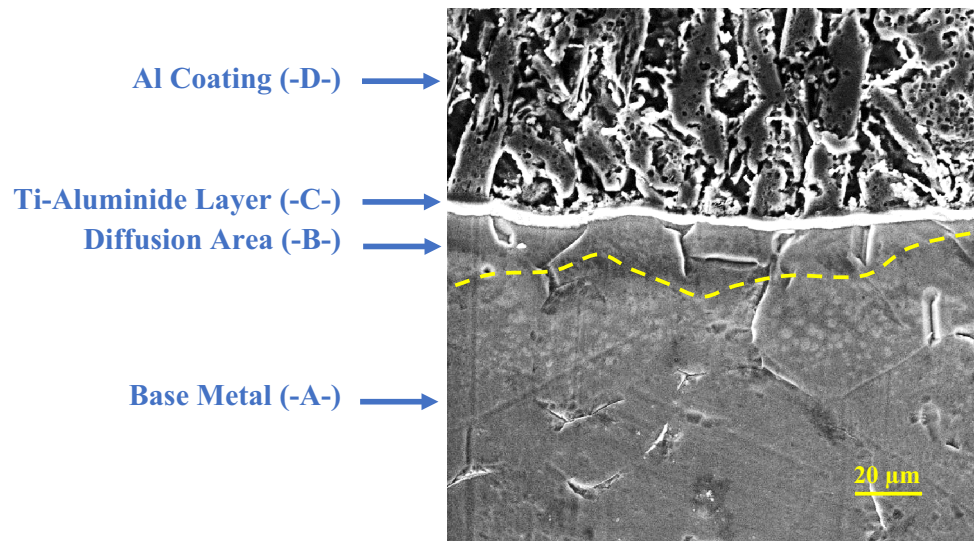
## 3 Results and Discussion

### 3.1 Microstructure Analysis of CP-Ti After H-DA Application

The cross section of a CP-Ti sample is shown in Fig. 2. In the process for the H-DA bath of Al 7075, the temperature was kept at 900 °C for 4 h. Figure 2 shows the three different layers of different thicknesses on the Ti [base metal (-A- in the image)] surface. This finding is consistent with the literature [26–29]. The top area, Al coating layer (-D- in the image), consisted of the Ti and Al. This layer was approximately 50  $\mu\text{m}$  thick. The Ti-aluminide layer (-C- in the image) formed on the Ti surface had a thickness of approximately 5  $\mu\text{m}$ . Moreover, the diffusion of Al (-B- in the image) was observed below the Ti-aluminide layer. The linear EDS analysis of the H-DA CP-Ti in Al 7075 at 900 °C for 4 h is shown in Fig. 3a, and the XRD analysis peaks are shown in Fig. 3b. The Ti concentration shown in Fig. 3a was determined at the 43-point number for Ti (main matrix), and then the Ti, Al, and O intensities were determined at the 43 to 100-point numbers for the Al-Ti phases. These intensities showed the pure Ti, TiAl, TiAl<sub>3</sub>, and Ti<sub>3</sub>Al peaks (Fig. 3b). Sujata et al. and Khoshhhal reported that the Ti<sub>3</sub>Al, TiAl, and TiAl<sub>3</sub> phases could be obtained by using a liquid H-DA technique with Ti as a base material [30, 31]. Although the Al coating and Ti-aluminide layers consisted of different amounts of Ti and Al elements, the concentration of Ti was generally higher (Fig. 3a). This situation was defined thermodynamically by

**Table 1** Chemical composition of Al 7075 alloy (wt%)

Cr	Cu	Fe	Mg	Mn	Si	Ti	Zn	Al
0.18–0.28	1.2–2	Max. 0.5	2.1–2.9	Max. 0.3	Max. 0.4	Max. 0.2	5.1–6.1	Balance

**Fig. 2** FESEM images of aluminized CP-Ti in Al 7075 at 900 °C for 4 h**Fig. 3** EDS and XRD analysis of aluminized CP-Ti in Al 7075 at 900 °C for 4 h

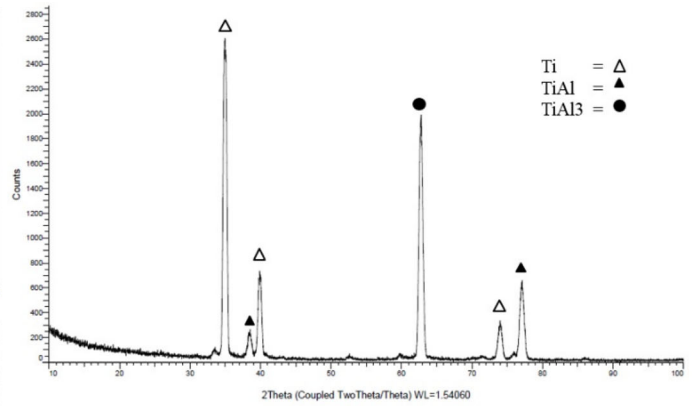
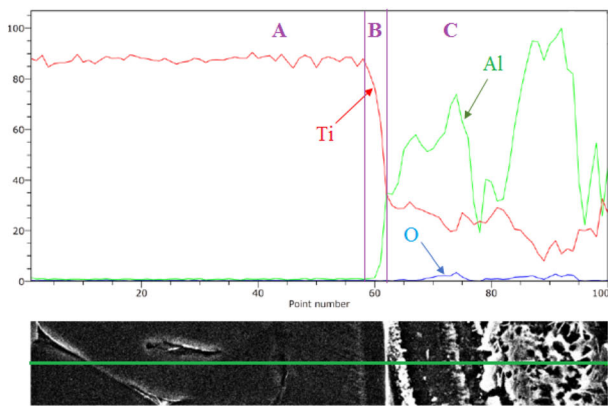
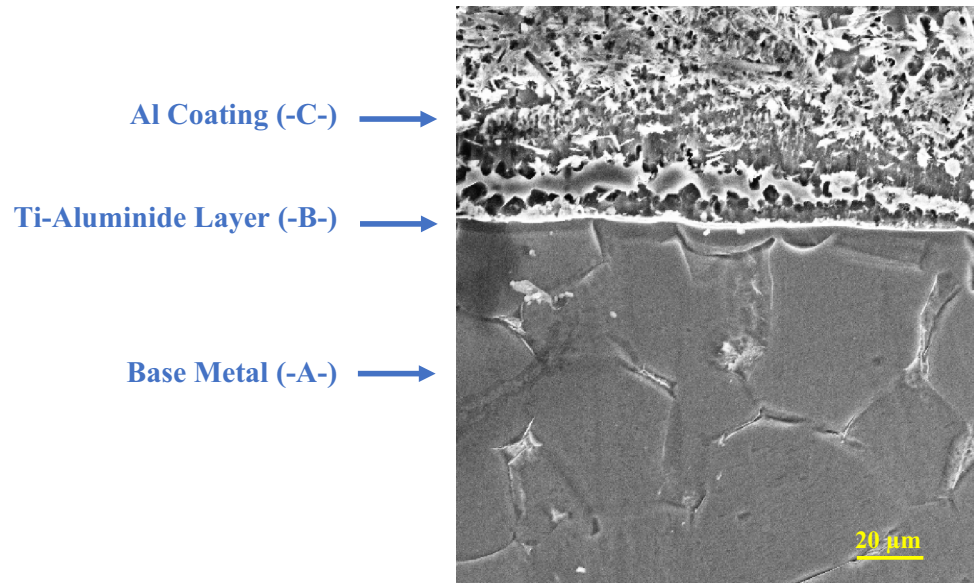
Kattner et al. [32] with the description of the Al diffusion in the Ti structure.

The FESEM image and EDS analysis of the CP-Ti after H-DA application in different media at constant temperature and time (900 °C and 4 h) are given in Figs. 4 and 5a, respectively, while Fig. 5b gives the XRD analysis peaks of the CP-Ti samples after H-DA application at 900 °C for 4 h. The H-DA process with the pure liquid Al environment resulted in a thinner aluminide layer than with the Al 7075 environment. Diffusion was not observed since the temperature and time were not sufficient for the H-DA process in the pure Al bath. In addition, a comparison of Figs. 2 and 4 shows a thicker aluminide layer for the Al7075 alloy than for the pure Al under equal H-DA

processing conditions (900 °C, 4 h). The reason could be that the alloying elements in Al 7075 served as activators, leading to a thicker Ti–Al layer. The XRD analysis in Fig. 5b shows the Ti, TiAl and TiAl<sub>3</sub> peak intensities. The peaks of TiAl<sub>3</sub> were determined to be between 900 °C and 1000 °C for pure liquid Al by Sujata et al. [33]. Here, the main peaks of the Ti, TiAl, and TiAl<sub>3</sub> were obtained with H-DA at 900 °C, as shown in Fig. 5b.

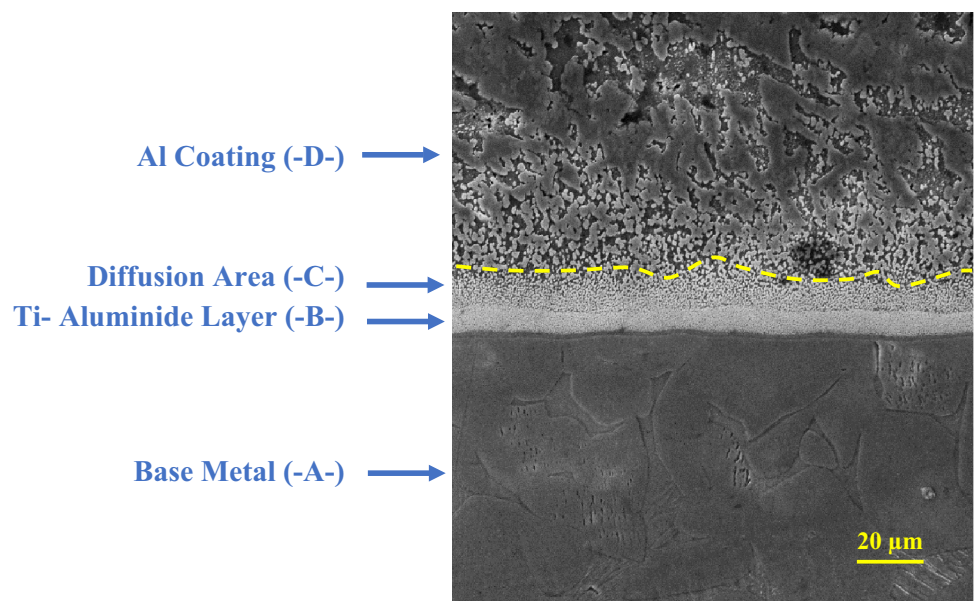
Figure 6 shows the FESEM image of a CP-Ti sample after H-DA application in liquid Al 7075 at 1000 °C for 4 h. Figure 7a shows the EDS analysis peaks and Fig. 7b the XRD analysis of the CP-Ti after H-DA application in liquid Al 7075 at 1000 °C for 4 h. In the FESEM image, the Al coating layer and diffusion area increased with the

**Fig. 4** FESEM images of aluminized CP-Ti in pure Al at 900 °C for 4 h



**Fig. 5** EDS and XRD analysis of aluminized CP-Ti in pure Al at 900 °C for 4 h

**Fig. 6** FESEM images of aluminized CP-Ti in Al 7075 at 1000 °C for 4 h



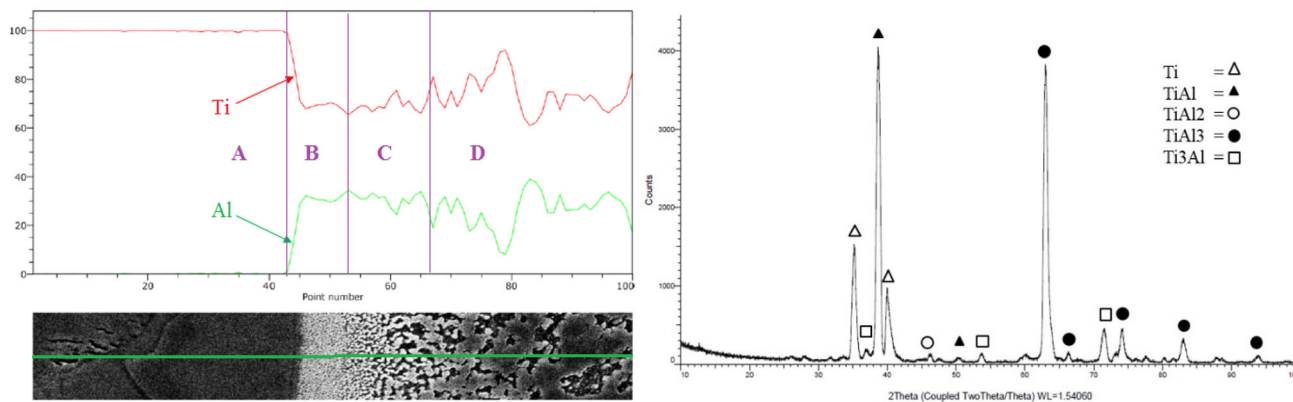


**Fig. 7** EDS and XRD analysis of aluminized CP-Ti in Al 7075 at 1000 °C for 4 h

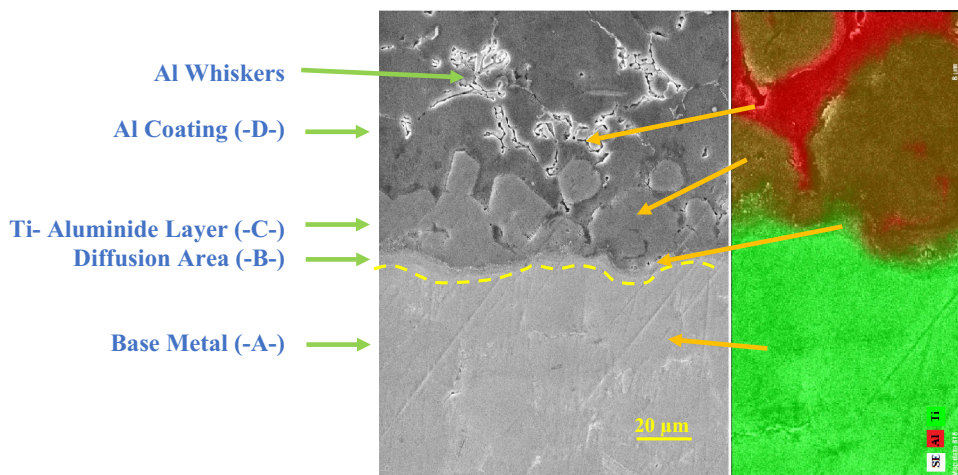
increase in the processing temperature to 1000 °C. At 900 °C, a thinner diffusion layer was obtained (Fig. 2). It was determined that the temperature affected the Ti–Al phases, and new phases were formed as TiAl<sub>2</sub> and Ti<sub>3</sub>Al. The obtaining of the Ti<sub>3</sub>Al [34, 35] and TiAl<sub>2</sub> [36] phases was a direct effect of the thermodynamic equilibrium resulting from the high temperature of the processing condition. At higher temperatures, the diffusion of Al might have led to the formation of Ti<sub>3</sub>Al, as it was observed in Ti alloys having an Al content of more than 5.5 wt% [34, 35]. In addition, EDS analysis results showed that the increased temperature prevented the formation of oxides and created an atmospheric protective cover on the liquid Al system.

In order to better understand the morphology involved with H-DA, the processing time was increased to 6 h and an elemental mapping analysis was performed on the FESEM image (Fig. 8). The EDS analysis results and XRD peaks of the CP-Ti after H-DA application in pure Al at 1000 °C for 6 h are shown in Fig. 9a, b, respectively. In the colored MAP image, the Ti was found to be green, the Al was red, and the Ti-aluminide layer was brown (a

mixture of green and red). Furthermore, the formation of the many TiAl<sub>3</sub> intermetallics in the microstructure gave the phase attractive physical, chemical, and mechanical properties which were detected in the XRD peaks. These intermetallics were near the grain boundaries and as such, served to improve the mechanical properties [27]. Thus, the MAP and XRD analyses apparently confirmed the formation of the Ti-aluminide phases TiAl, TiAl<sub>2</sub>, TiAl<sub>3</sub>, and Ti<sub>3</sub>Al on the CP-Ti surface via the H-DA process.

The obtained findings are tabulated in Table 2 for summarizing all experimental results. All microstructure analyses are summarized as a table to avoid the confusion of many images. The effect of temperature, process time, and aluminizing bath are clearly seen in Table 2. Increasing the processing temperature and time led to thicker Ti-aluminide layers. Higher temperatures increased the energy, and therefore, the movement of the molecules increased the rate of diffusion. The increase in the diffusion rate caused an increase in the layer thickness. Likewise, increasing the process time led to thicker Ti-aluminide layers because of the increased diffusion time.

**Fig. 8** FESEM image and MAP analysis of aluminized CP-Ti in pure Al at 1000 °C for 6 h



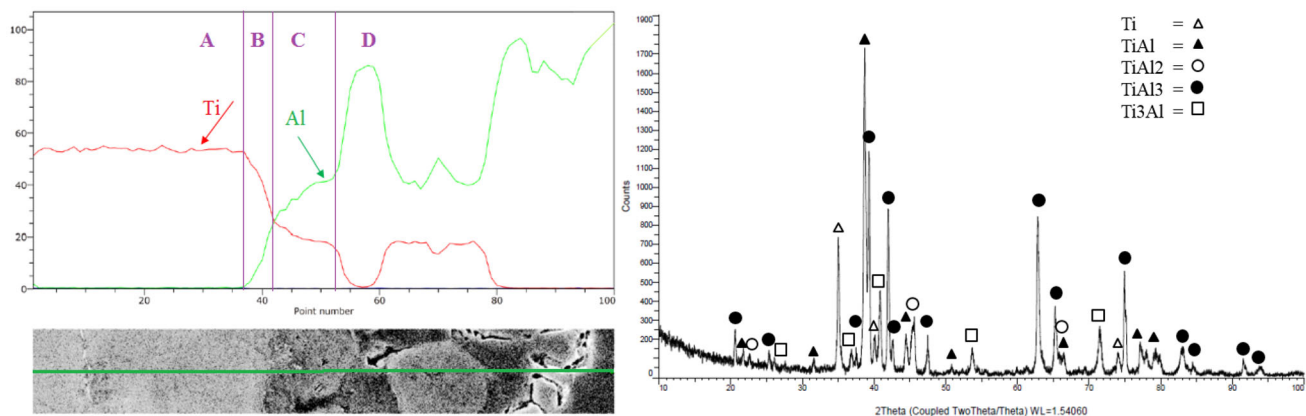


**Fig. 9** EDS and XRD analysis of aluminized CP-Ti in pure Al at 1000 °C for 6 h

**Table 2** Summary of microstructure analyses after the H-DA process

Temperature (°C)	Time (h)	Bath	Layer observed	Thickness	Composition
900	4	Pure Al	Al coating	80 μm	TiAl
			Ti-aluminide	3 μm	TiAl <sub>3</sub>
900	4	Al 7075	Al coating	50 μm	TiAl
			Ti-aluminide	5 μm	TiAl <sub>3</sub>
			Diffusion area	25 μm	Ti <sub>3</sub> Al
900	6	Pure Al	Al coating	80 μm	TiAl
			Ti-aluminide	5 μm	TiAl <sub>2</sub> TiAl <sub>3</sub>
900	6	Al 7075	Al coating	65 μm	TiAl
			Ti-aluminide	8 μm	TiAl <sub>3</sub>
			Diffusion area	25 μm	Ti <sub>3</sub> Al
1000	4	Pure Al	Al coating	50 μm	TiAl
			Ti-aluminide	15 μm	TiAl <sub>3</sub>
			Diffusion area	10 μm	Ti <sub>3</sub> Al
1000	4	Al 7075	Al coating	90 μm	TiAl
			Ti-aluminide	10 μm	TiAl <sub>2</sub>
			Diffusion area	15 μm	TiAl <sub>3</sub> Ti <sub>3</sub> Al
1000	6	Pure Al	Al coating	65 μm	TiAl
			Ti-aluminide	22 μm	TiAl <sub>2</sub>
			Diffusion area	5 μm	TiAl <sub>3</sub> Ti <sub>3</sub> Al
1000	6	Al 7075	Al coating	60 μm	TiAl
			Ti-aluminide	30 μm	TiAl <sub>2</sub>
			Diffusion area	10 μm	TiAl <sub>3</sub> Ti <sub>3</sub> Al

### 3.2 Microhardness Analysis of CP-Ti After H-DA Application

Microhardness of samples was determined by the Vickers testing method using a 136° pyramidal diamond indenter.

The applied load was 100 g with 10 s dwell time using the Hardway DV-1AT-4.3 hardness tester. The different heat treatments were investigated by comparing microhardness, and thereby the different microstructures. Four different areas were measured for microhardness assessment, as

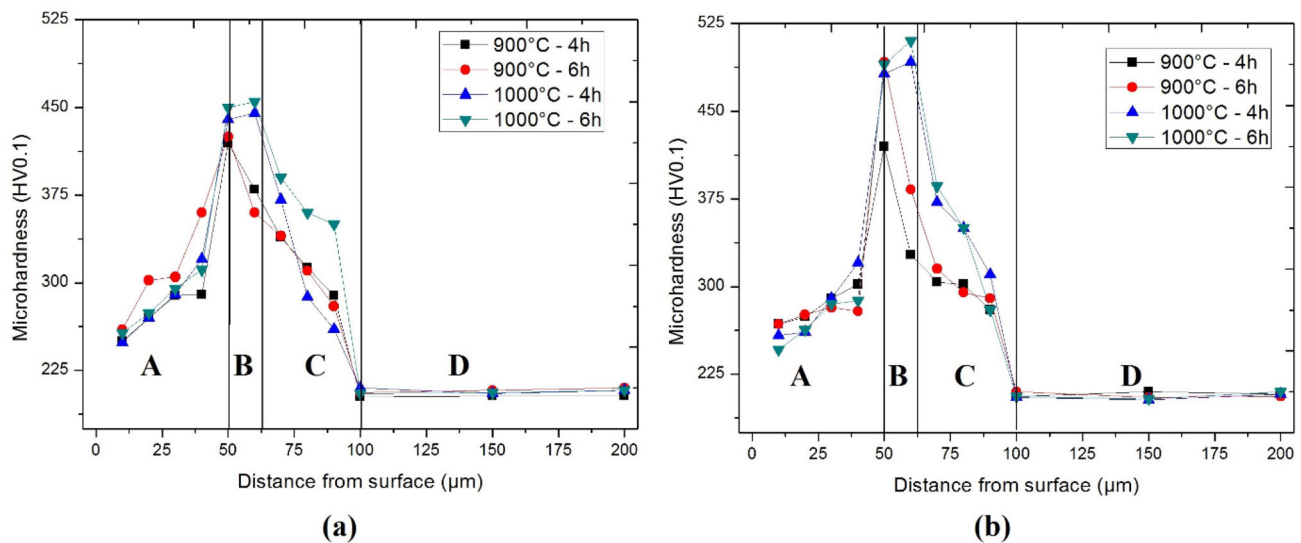


**Fig. 10** Microhardness profile of aluminized CP-Ti in **a** pure Al, **b** Al 7075

shown in Fig. 10a, b. The findings were consistent with the microstructural analysis. The Al coating (-A- in the graph) had higher hardness than the base metal with 200 HV. The Ti-aluminide layer (-B- in the graph) had a higher hardness value on the surface. Up to 100  $\mu\text{m}$ , the hardness value gradually decreased in the diffusion area (-C-). After 100  $\mu\text{m}$ , the hardness became equal to the hardness of the base metal for both the pure Al and Al 7075 baths. The hardness values of CP-Ti after H-DA in Al 7075 were found to be higher than with H-DA in pure Al. The highest hardness value in all experiments was obtained as 510 HV for samples aluminized in an Al 7075 bath at 1000  $^{\circ}\text{C}$  for 6 h. The increasing of the hardness values could be described as obtaining the phases of  $\text{Ti}_3\text{Al}$ , Ti-rich TiAl, Al-rich TiAl, and  $\text{TiAl}_3$  that were all harder than the main structure (pure Ti) [37]. Thus, the harder phases such as  $\text{Ti}_3\text{Al}$  [38],  $\text{TiAl}_3$  [39, 40], and TiAl were between the areas of A and C. The microhardness in these phases was increased by grain refinement and the border effects at the grain boundaries [41]. The alloy elements in the Al 7075 increased its hardness value (Fig. 10b), which was higher than that of pure Al (455 HV). Thus, the Al 7075 led to finer grains and more grain boundaries than the pure Al [42].

## 4 Conclusions

This paper presented the results of the microstructure analysis of aluminized CP-Ti, which used H-DA to form Ti-aluminides on the surface. The results showed that H-DA is an extremely low-cost method of forming Ti-

aluminides compared to other aluminizing techniques. The following conclusions were reached:

- Increasing the H-DA processing temperature and time resulted in a thicker aluminide layer and diffusion area. The optimum temperature and process time were 1000  $^{\circ}\text{C}$  and 6 h for all the H-DA process results.
- Applying the H-DA process at 900  $^{\circ}\text{C}$  with Al 7075 resulted in Ti, TiAl,  $\text{TiAl}_3$ , and  $\text{Ti}_3\text{Al}$  phases that were finer and diffused homogeneously within the matrix.
- H-DA processing at 1000  $^{\circ}\text{C}$  for 6 h resulted in the formation of the Ti, TiAl,  $\text{TiAl}_3$ , and  $\text{Ti}_3\text{Al}$  phases.
- The hardness values were increased at the Al diffusion area because of the TiAl,  $\text{TiAl}_3$ , and  $\text{Ti}_3\text{Al}$  phases.
- Increasing the processing temperature resulted in higher hardness values due to the increase in the harder TiAl,  $\text{TiAl}_3$ , and  $\text{Ti}_3\text{Al}$  phases.
- The alloy system was useful for increasing the hardness values and provided deeper diffusion than the pure metal system.
- The highest hardness values were obtained with the Al7075 alloy at 1000  $^{\circ}\text{C}$  for 6 h.

## References

1. Kaplan Y, Can A C, Ulukoy A, *P I Mech Eng. L-J Mat* **233** (2019) 109.
2. Viteri V S, Elena F, *Titanium and titanium alloys as biomaterials*, Rijeka: Intech, (2013), p 160.
3. Fenghua L, Xiaohong Y, Jinglei Z, Zhanguo F, Dianting G, Zhengping X, *Acta Metall Sin* **23**, (2010), 293.
4. Ataibis V, Taktak S, *Surf Coat Tech* **279** (2015) 65.

5. Donachie, M J, *Titanium: a technical guide*. Materials Park, OH: ASM International (2000), p 65.
6. Boyer R R, *Adv Perform Mater* **2** (1995) 349.
7. Ranjan S, Mukherjee B, Islam A, Pandey K K, Gupta R, Keshri A K, *J Eur Ceram Soc* **40** (2020) 660.
8. Sienkiewicz J, Kuroda S, Murakami H, Araki H, Giżyński M, Kurzydłowski K J, *J Therm Spray Techn* **28** (2019) 563.
9. Swadźba R, Swadźba L, Mendala B, Witala B, Tracz J, Marugi K, *Intermetallics* **87** (2017) 81.
10. Choi K, Song Y, Yi S, Park J S, *Korean J Met Mater* **57** (2019) 131.
11. Fan X, Darut G, Planche M P, Feng X, Liao H, Montavon G, *J Therm Spray Techn* **28** (2019) 265.
12. Esmaeili M M, Mahmoodi M, Imani R, *Int J Appl Ceram Tec* **14** (2017) 374.
13. Cammarota G P, Casagrande A, Sambogna G. *Surf Coat Tech* **201** (2006) 230.
14. Abro M A, Hahn J, Lee D B, *Met Mater Int* **24** (2018) 507.
15. Abro M A, Lee D B, *Met Mater Int* **23** (2017) 92.
16. Kim M J, Lee D B, *Korean J Met Mater* **53** (2015) 406.
17. Cheng W J, Wang C J, *App. Surf Sci* **257** (2011) 4663.
18. Wang C J, Badaruddin M, *Surf Coat Tech* **205** (2010) 1200.
19. Eaton D C G, *Advanced Materials for Lightweight Structures*, in: Proceedings of the ESA International Symposium, ESA SP-339.
20. Nouri S, Rastegari S, Mirdamadi S, Hadavi M, *Trans Indian Inst Met* **68** (2015) 867.
21. Kothari K, Radhakrishnan R, Wereley N M, *Prog Aerosp Sci* **55** (2012) 1.
22. Cahn R W, Haasen P, *Physical Metallurgy*, 4th ed. Elsevier, Amsterdam, (1996).
23. Whang S H, Pope D P, Liu C T, *High temperature aluminides and intermetallics*, in: Proceedings of the 2nd ASM Conference on HTAAI, Elsevier, Amsterdam, (1993).
24. Medda E, Delogu F, Cao G. *Mat Sci Eng A* **361** (2003) 23.
25. Gupta RK, Pant B, Sinha P P, *Trans Indian Inst Met* **67** (2014) 143.
26. Jiang W, Fan Z, Li G, Liu X, Liu F, *J Alloy Compd* **688** (2016) 742.
27. Rastkar A R, Parseh P, Darvishnia N, Hadavi S M M, *Appl Surf Sci* **276** (2013) 112.
28. Hafitlang F, Habibolahzadeh A, Sohi M H, *App. Surf Sci* **329** (2015) 240.
29. Kim J H, Wang J P, Kang C Y, *Met Mater Int* **17** (2011) 931.
30. Khoshhal R, *Met Mater Int* **25** (2019), 449.
31. Sujata M, Bhargava S, Sangal S J, *J Mater Sci Let*, **1** (1997) 1175.
32. Kattner U R, Lin J C, Chang Y A, *Metall Trans A* **23** (1992) 2081.
33. Sujata M, Bhargava S, Sanga S, *ISIJ Int*, **36** (1996) 255.
34. Loo F J, Rieck G D, *Acta Metall* **21** (1973) 73.
35. Sprengel W, Nakajima H, Oikawa H, *Mat Sci Eng A* **213** (1996) 45.
36. Loiseau A, Vannuffel C, *Phys Status Solidi A* **107** (1988) 655.
37. Mizuta N, Matsuura K, Kirihara S, Miyamoto Y, *Mat Sci Eng A* **492** (2008) 199.
38. Jianing L, Chuanzhong C, Lei Z, *Int. J. of Refract. Met H* **29** (2011) 49.
39. Li S, Ling-Yan K, Tian-ying X, Hao D, Tie-fan L, *Trans Non-ferrous Met Soc China* **19**, (2009) 879.
40. Udayashankar N K, Rajasekaran S, Nayak J, *Trans. Indian Inst. Met.* **61** (2008) 231.
41. Jianing L, Chuanzhong C, Zhaoqing L, Squartini T, *J Alloy Compd* **509** (2011) 4882.
42. Venkataraman B, Sundararajan G, *Wear* **245** (2000) 22.

**Publisher's Note** Springer Nature remains neutral with regard to jurisdictional claims in published maps and institutional affiliations.